ELSEVIER

Polymer 41 (2000) 3253–3262

polymer

X-ray photoelectron spectroscopy study of electrically conducting polyaniline/polyimide blends

Moon Gyu Han, Seung Soon Im*

Department of Textile and Polymer Engineering, Graduate School of Advanced Material and Chemical Engineering, Hanyang University, 17 Haengdang-dong, Seungdong-gu, Seoul 133-791, South Korea

Received 16 February 1999; received in revised form 23 June 1999; accepted 7 July 1999

Abstract

The changes in protonation level ($[N^+]/[N]$ ratio), doping state, and conjugation condition for polyaniline-complexes/polyamic acid (PANI-complexes/PAA) blends and their thermally cured polyaniline-complexes/polyimide (PANI-complexes/PI) have been assessed by X-ray photoelectron spectroscopy and UV–Vis spectroscopy. It was suggested that the protonation levels were predominantly associated with dopants that show different protonation ability. By XPS N1s peak convolution, it was found that thermal treatment of blends led to dedoping when the curing temperature reached 250°C. However, stability of protonation state of blends against thermal curing was higher than pure PANI-complexes. Dopants in the blends also affect the distribution of N^+ species and thermal stability to curing. Mild thermal treatment (180°C) led to the increase of conjugation length ascribing to the increased order of polymer chain, although their protonation levels were not increased.

Keywords: Conductive polymer blends; Polyaniline; Polyimide

1. Introduction

Recent innovating means for increasing processability of polyaniline (PANI) was counterion-induced processability with functionalized protonic acids like camphorsulfonic acid and dodecylbenzenesulfonic acid [1,2]. By these dopants, solutions or melts of PANI-complexes in the conducting form with high conductivity could be obtained. Because the conducting forms of PANI are inherently brittle, on the contrary, efforts to improve the mechanical properties and broaden the range of industrial applications have been directed toward blending with other polymers. In the view of enhancing the mechanical properties and thermal stability of conductivity, the blends of PANI and polyimide (PI) have been prepared and reported [3,4]. The electrical conductivity, blends behavior and the structure of the blends were investigated in these papers.

PANI have a general formula $[(-B-NH-B-NH-)_y(-B-N=Q=N-)_{1-y}]_x$, in which B and Q denote the C_6H_4 rings in the benzenoid and quinoid forms, respectively [5,6]. The intrinsic oxidation state of PANI can range from that of the fully oxidized pernigraniline ($y = 0$), through that of 50% oxidized emeraldine ($y = 0.5$), to that of fully reduced leucoemeladine ($y = 1$). PANI can achieve its highly conductive state either through the protonation of the imine nitrogens (=N–) in its emeraldine state, or through the oxidation of the amine nitrogens (–NH–) in its fully reduced leucoemeraldine state [6,7]. Because X-ray photoelectron spectroscopy (XPS) measurement is a good way to determine quantitatively proportions of quinoid imine, benzenoid amine and positively charged nitrogen in PANI, many researchers reported the intrinsic protonation states by this method [8–11]. But, little is known about the change of XPS spectra and the blend behavior of PANI-complexes when it was blended with other host polymers.

The idea of this paper is that the protonation states of PANI-blends can be quantitatively analyzed by XPS measurement. The positively charged nitrogen portion is related to the doping level, in other words protonation level of the blends, which plays an important role in electrical conductivity. On the contrary, because our blend system is composed of various imidization states, viz. different thermal cured states, investigations of the change of nitrogen species by varying the thermal curing step could be important in evaluating and analyzing the variation of the internal structure of the blends. Hence, the XPS study of the PANI/PI films with various curing steps is described here together with UV–Vis spectra and conductivity measurement.

* Corresponding author. Tel.: +82-2-2290-0495; fax: +82-2-2297-5859.
E-mail address: imss007@email.hanyang.ac.kr (S.S. Im).

0032-3861/00/$ - see front matter
PII: S0032-3861(99)00531-5

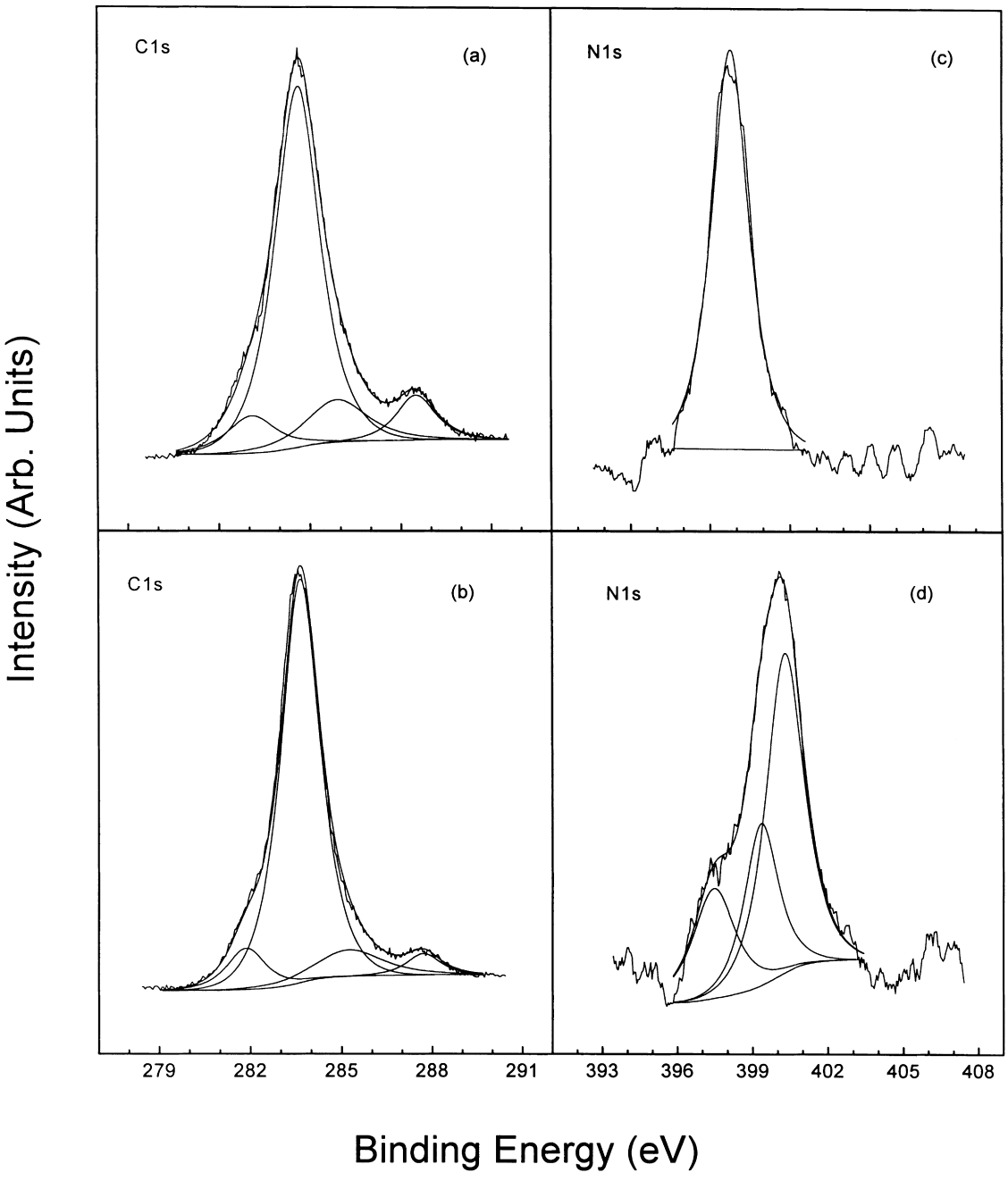

Fig. 1. C1s core-level spectra of (a) PAA and (b) PI, and the N1s core-level spectra of (c) PAA and (d) PI. The raw data (jagged curve) have been deconvoluted into Gaussian/20% Lorentzian peaks on a Shirley background.

2. Experimental

The PANI-complex/PAA blends were prepared by the reported method [3,4]. The sample name C50 and D50 means 50 wt.% PANI-CSA and PANI-DBSA blends, respectively. The attached numbers located after the hyphen are the curing temperatures. The intrinsic oxidation state and protonation levels of blend films were determined by XPS. The XPS measurements were made on a SSI, 2803-S spectrometer with Al K_α X-ray source. The X-ray source was 12 kV and 20 mA. All core-level spectra were obtained at a photoelectron take-off angle of 35° with respect to the sample surface. The peaks were deconvoluted into the components consisting of a Gaussian line shape Lorentzian function (Gaussian:80%, Lorentzian:20%) on a Shirley background. To compensate for the surface charging effect, all binding energies were referenced to C1s neutral carbon peak at 284.6 eV. The elemental stoichiometries were determined from the peak area ratio, after correcting with the sensitivity factors. The electrical conductivity of the blend films was measured using the standard four-probe method, and for measuring the conductivity variation with

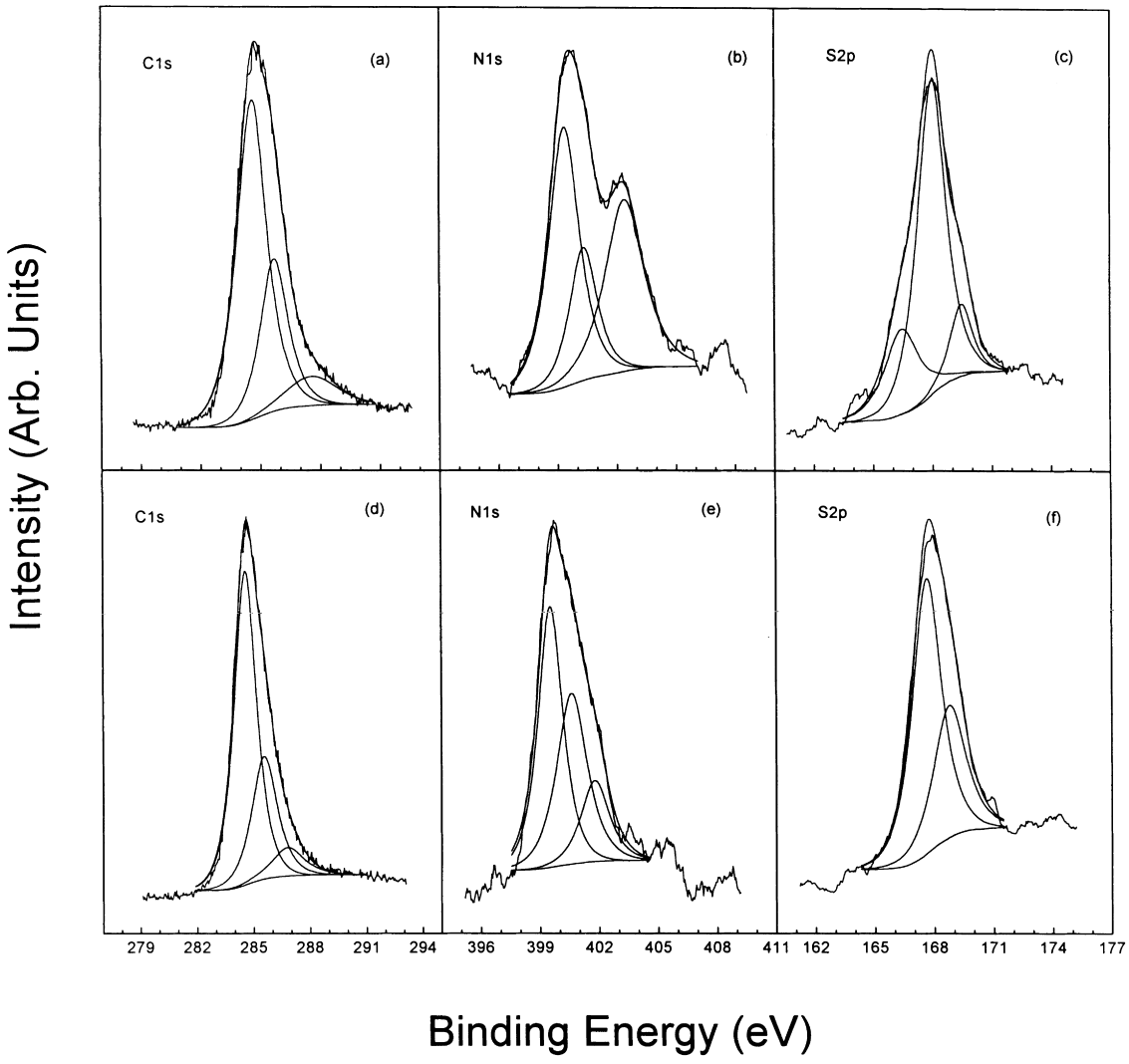

Fig. 2. XPS narrow scans of PANI-CSA ((a), (b), (c)) and that of PANI-DBSA ((d), (e), (f)).

temperature the four-probe cell was inserted in a glass tube. UV–Vis absorption spectra of the films coated on the ITO glass followed by thermal curing were recorded with an UNICAM 8700 series UV–Vis spectrophotometer.

3. Results and discussion

Fig. 1(a) and (b) shows Cls core-level spectra of PAA and PI, respectively. The C1s peak of PAA was fitted with four components: at 283.09 eV (C–H species), at 284.6 eV (C–C species), at 285.94 eV (C–N or C–O species), and at 288.54 eV (C=O species) [12]. The spectrum of C1s core-level of PI has a similar shape except shifting of each component and changing of area ratio of respective species: 281.88 eV (phenyl carbon (ODA) bonded to hydrogen), at 284.6 eV (phenyl carbon (PMDA), C–C or C–N species), at 285.28 eV (C–O species), and at 287.73 eV (C=O species (carbonyl carbon)). The portion of the third peak (C–O species) of PI revealed at 285.28 eV decreases in comparison with that of PAA (285.94) from 11.6 to 8.7% by area. It means the transformation of the carboxyl group into the carbonyl group by cyclization (imidization) with elimination of water. The shapes of the N1s core-level spectra of two samples are different in Fig. 1(c) and (d). PAA shows only one peak at 399.5 eV which are attributed to the N species (C–N–C) that could not form the cyclic imide ring. The spectrum of PI has three species, 397.58, 399.38, and 400.33 eV, respectively, for imine nitrogen, N species from PAA, and imide nitrogen. This result also suggests that PAA was converted to PI after the thermal imidization process. There may be a possibility of the existence of oxidized or protonated N atoms. From these peak deconvolutions, however, the oxidized or protonated N atoms on doping seem to be absent. It seems hardly possible that N atoms of the amide group in PAA and those of the imide in PI have the reactivity with dopants because nitrogen of amide group or imide ring exist in the main chain of polymers with a rigid aromatic backbone.

XPS spectra (C1s, N1s, S2p) of PANI-CSA and

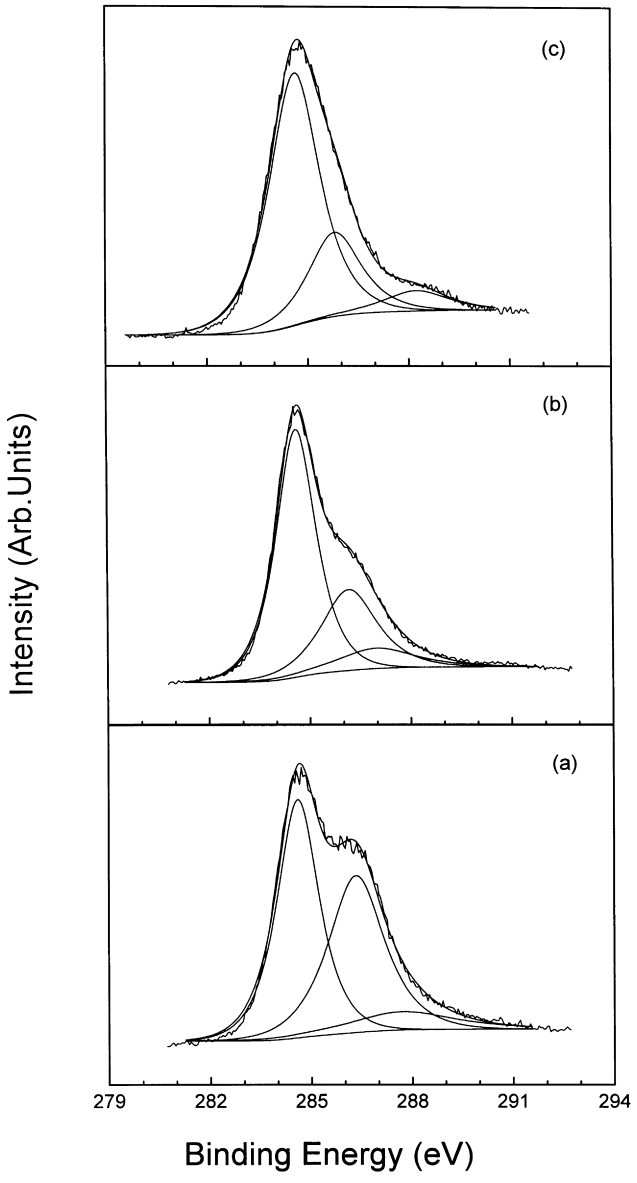

Fig. 3. C1s core-level spectra of: (a) C50; (b) C50-180; and (c) C50-250.

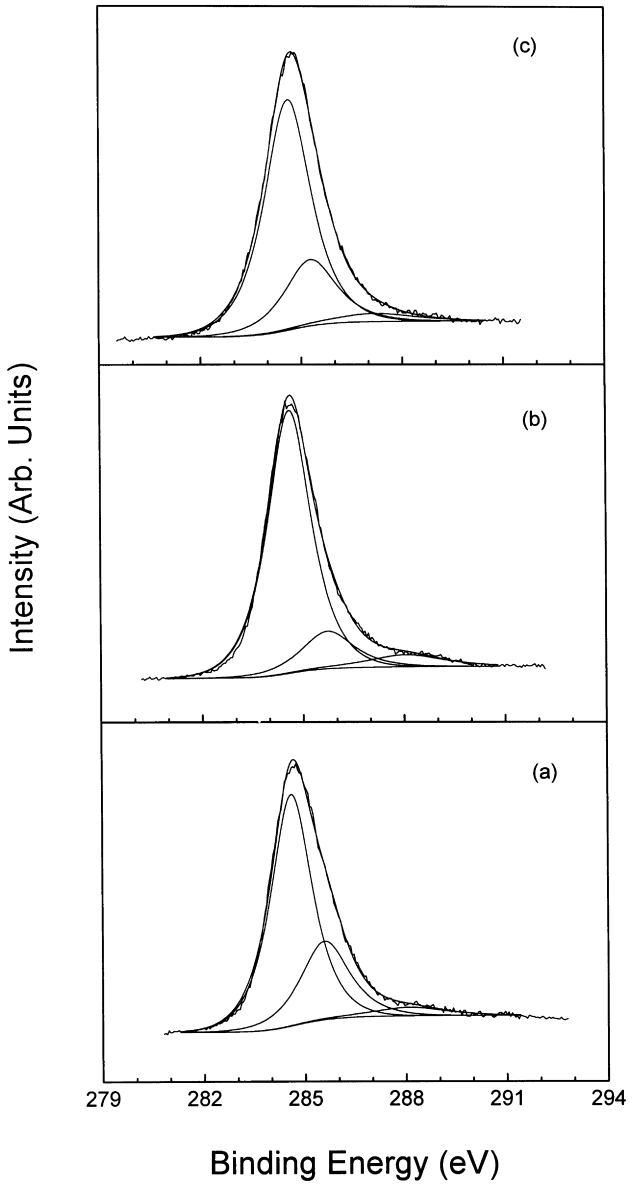

Fig. 4. C1s core-level spectra of: (a) D50; (b) D50-180; and (c) D50-250.

PANI-DBSA were shown in Fig. 2. The C1s spectrum of PANI-CSA can be deconvoluted into three environments: C–C or C–H at 284.6 eV, C–N or C=N at 285.7, C–N^+, C=N^+ or C=O at 287.6. Small, high binding energy (BE) tails (BE = 287.6 eV) due to the π–π^* bonding band which is a long-range order with a polymer chain shake-up satellite structure coincide with the well-doped state. PANI-DBSA was also deconvoluted with three peaks at 284.6, 285.65, 286.95 eV by matching the same component as PANI-CSA [13]. In general, quinoid imine, benzenoid amine, and positively charged nitrogen in the PANI-complex correspond, respectively, to N1s core-level peak components revealed at about 398, 399 and over 400 eV in the curve-fitted N1s core-level spectrum [14]. In PANI-CSA, –NH– from benzenoid amine is revealed at 399.35 eV and the N^+ species appeared in two peaks at 400.35 and 402.4 eV. The –NH– species is located at 399.53 eV and two N^+ peaks are shown at 400.63 and 401.78 eV, respectively, in PANI-DBSA. The most important feature is the difference in distribution of the N^+ species and the [N^+]/[N] ratios (N: sum of –N=, –NH–, N^+) in two PANI-complexes. In both complexes, all the imine nitrogens were protonated and transformed into the positively charged nitrogens, consistent with the fact that protonation occurred preferentially at the imine nitrogens [15,16]. However, the proportion of positively charged nitrogens exceeded 50%, suggesting that additional protonation occurred at the amine nitrogens [17]. It can be suggested that protonation in the amine site of PANI would lead to the –N^+H_2– groups. This would probably reduce the extent of the π-conjugation and thus bring about more uniform positive charges on the polymer chain [17]. The different shape of the N1s spectra suggests that

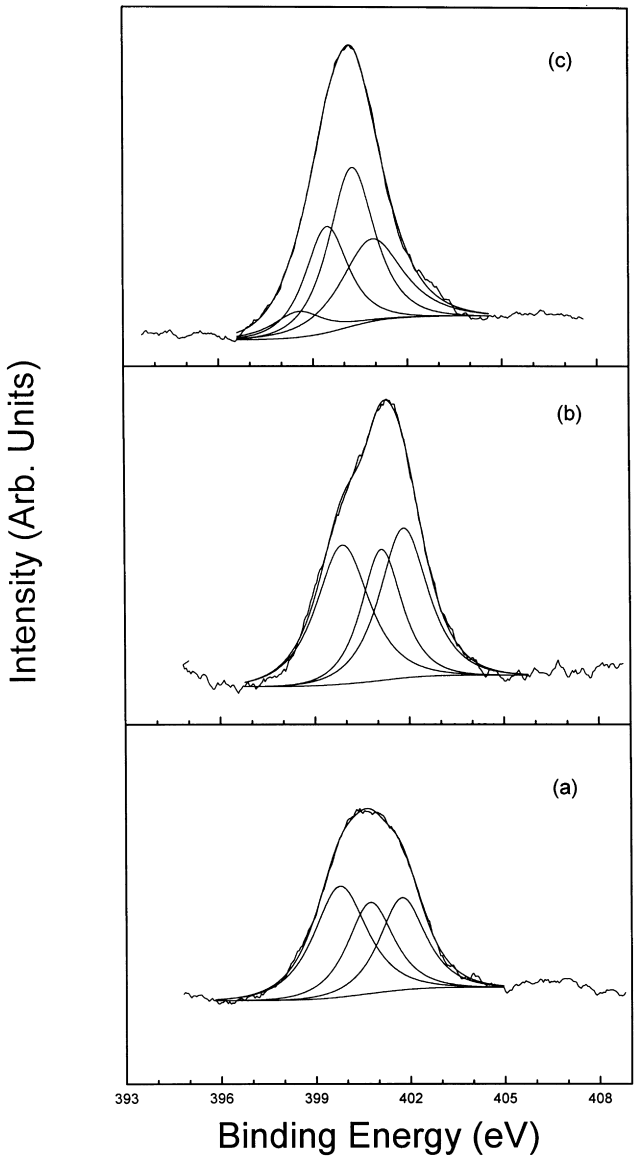

Fig. 5. N1s core-level spectra of: (a) C50; (b) C50-180; and (c) C50-250.

these two PANI-complexes have dissimilar distribution of N^+ species, in other words, different doping states. These two peaks can be assigned to the $-NH^+$ radical-cation and to the imine cation $=NH^+$, which are related to polaron and bipolaron, respectively, [18,19]. The difference in the shape of the high BE tail of the PANI-DBSA, as compared with PANI-CSA, suggests some difference in the electrostatic interaction of the anions with PANI. This may be the result of the geometric difference of anions, proton donating ability divergence, or difference in complex formation morphology in the solution. Generally, the shape of the N1s spectra of PANI-CSA is characteristic of heavily protonated PANI [17]. It thus suggests higher protonation of PANI-CSA than PANI-DBSA. The S2p core-level signal attributed to the covalently bonded sulfate anion ($-SO_3^-$) can be fitted with the spin–orbit doublet $S(2p_{3/2})$ and $S(2p_{1/2})$ [20] lying at about 167.7 and 168.8 eV, respectively, in PANI-DBSA. But, PANI-CSA could be deconvoluted with three peaks adding one small peak at 166.5 eV to the existing peaks at around 167.9 and 169.5 eV. The appearance of a low-BE S2p peak indicates that a fraction of sulfate anions in PANI-CSA exists in more electron-rich conditions [21], which means that PANI doped by CSA have higher doping state than DBSA due to difference of geometry or the protonating ability of dopants.

Figs. 3 and 4 show C1s spectra of CSA- and DBSA-doped blends, respectively. The shapes of the two blends are different in nature. In Fig. 3, C1s spectrum of CSA-doped blends can be deconvoluted into three environments: C–C or C–H at 284.6 eV, C–N or C=N at 285.83 ~ 286.36, $C-N^+$, $C=N^+$ or C=O at over 287.8. The second peaks located from 286.36 (C50) to 285.83 (C50-250) have the tendency to reduce with thermal curing conditions. The extraordinarily high intensity of the second peak exists characteristically in only CSA-doped blends. This peak was diminished as the curing temperature increased. The reason for the high intensity of this peak and the reduction of peak intensity with the curing steps are uncertain. Small high BE tails (BE $>$ 287.8 eV) core-level spectra due to the $\pi-\pi^*$ bonding band agree with the well-doped state irrespective of the thermal curing step. C1s spectra of DBSA-doped blends were also deconvoluted with three peaks (Fig. 4). The high BE tail over 288 eV of Fig. 4(a) was also preserved regardless of thermal curing.

Fig. 5(a) shows the N1s core-level spectrum for CSA-doped blends prepared from the NMP solution without thermal curing. In this case, benzenoid amine (–NH–) and

Table 1
XPS results of relative atomic concentration (%)

Sample	C1s		O1s		N1s		S2p	
	Calc.[a]	Meas.[b]	Calc.	Meas.	Calc.	Meas.	Calc.	Meas.
PANI-CSA	75.86	75.34	13.79	13.81	6.90	6.92	3.45	3.93
C50	73.35	72.96	18.31	18.32	6.67	6.72	1.67	2.08
PANI-DBSA	83.33	81.86	8.33	9.17	5.56	5.48	2.78	3.49
D50	77.02	76.80	15.61	15.38	6.01	5.97	1.36	1.85

[a] Calculated value.
[b] Measured value after correction with the sensitivity factor.

Table 2
N1s data of various samples from XPS results

Sample	N1s binding energy (eV)			Proportion (%)[a]			
	–N=	–NH–	N^+	–N=	–NH–	N^+	S/N[b]
PANI-CSA		399.35	400.35, 402.4		45.5	56.7	0.568
C50		399.8	400.75, 401.75		42.3	57.7	0.310
C50-180		399.92	401.12, 401.82		37.3	62.7	0.289
C50-250	398.63	399.48	400.28, 400.93	7.2	25.2	67.6	0.246
PANI-DBSA		399.53	400.63, 401.78		46.4	53.6	0.637
D50		399.41	400.11, 401.22		49.3	50.7	0.310
D50 − 180		399.24	400.09, 401.04		51.1	48.9	0.294
D50-250	398.82	399.57	400.52, 401.47	8.9	24.2	66.9	0.217

[a] Determined from the curve-fitted N1s core-level spectra.
[b] Determined from the corrected S2p and N1s core-level spectral area ratio.

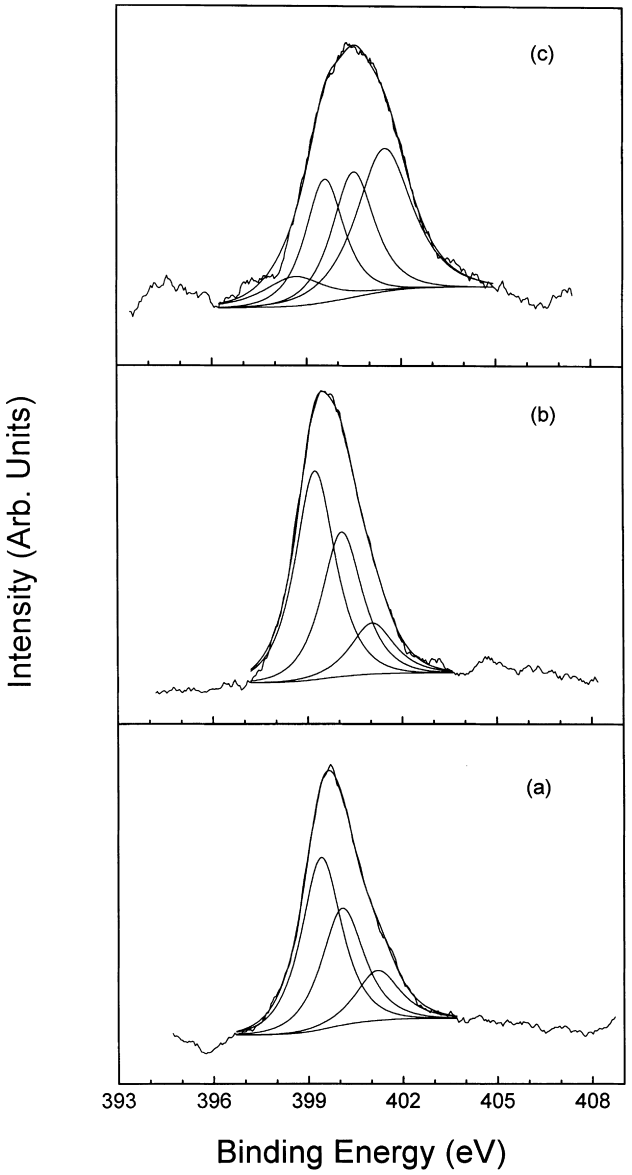

Fig. 6. N1s core-level spectra of: (a) D50; (b) D50-180; and (c) D50-250.

positively charged nitrogens of PANI are revealed at 399.8 and >400 eV, respectively. The high BE tail in the N1s spectrum, attributable to the protonated (positively charged) nitrogens, has been resolved into two peaks separated by about (0.95) and (1.95) from the amine peak, respectively. Fig. 5(b) shows a phase similar to Fig. 5(a). But, Fig. 5(c) could be deconvoluted into four peaks by adding the peak at low binding energy (398.63 eV) which arise from quinoid imine (=N–). This suggested that C50 had undergone the thermal dedoping process during curing at 250°C. Detailed peak data are listed in Tables 1 and 2. The N1s core-level spectra of D50 blends were shown in Fig. 6. Quinoid imine (=N–), benzenoid amine (–NH–) and positively charged nitrogens (N^+) of PANI are revealed at 399.82, 399.57 and >400 eV, respectively. As with the CSA-doped blends, the quinoid imine spectra at <399 eV was revealed (Fig. 6(c)). However, the shape of the N1s core-level spectra is different from CSA-doped blends. The difference in the distribution of two N^+ spectra of blends seems to be ascribed to pure PANI-CSA and PANI-DBSA, which have different doping states from one another.

Relative atomic percentage of PANI-complexes and their blends after correcting with the sensitivity factors are listed in Table 1. The calculated atomic percentages of PANI-complexes were computed by number of atoms in the polymer. It was calibrated by multiplying the PAA component with the proper constant for the purpose of calculating the atomic number in the blends by considering the mole fraction of two components, because the weight content of PANI-complexes was maintained to 50 wt.%. The measured atomic percentage obtained from the sensitivity factor correcting of each component was close to the calculated value with the exception of sulfur content. The reason for the extra high content of sulfur in comparison with the calculated value is due to excess introduction of dopants to block the insufficient doping of both PANI-complexes and to increase solubility, especially for PANI-DBSA. Therefore, when comparing theoretical S/N ratios (sulfur to nitrogen ratios) of PANI-complexes (50%) with the measured values which are calculated by dividing the N1s

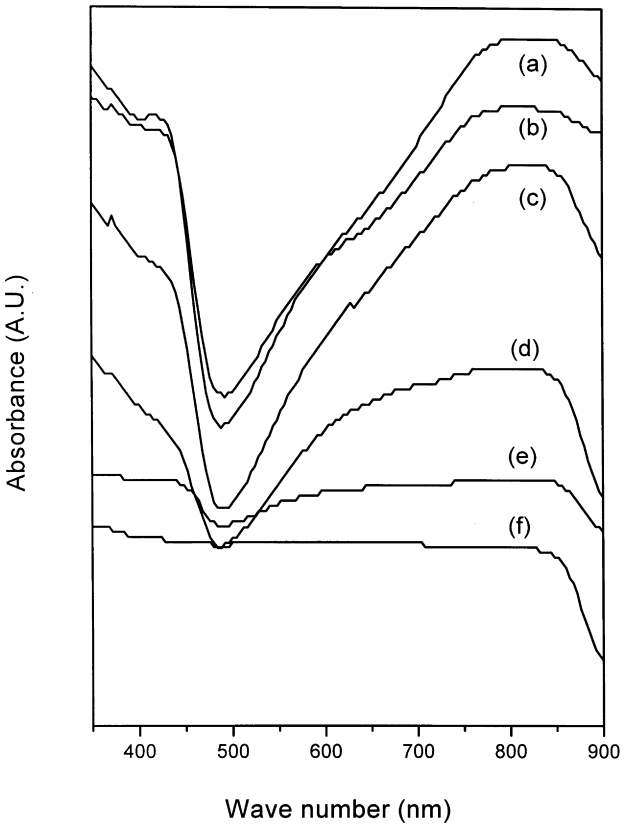

Fig. 7. UV–Vis spectra of PANI-CSA, and the same material such as those of cured samples: (a) up to proper temperature; (b) 120°C; (c) 150°C; (d) 180°C; (e) 210°C; and (f) 250°C.

percentage with S2p percentage in Table 1, it appears that PANI-CSA (56.8%) and PANI-DBSA (63.7%) have excess S/N value.

The N1s spectra obtained from Figs. 5 and 6 and the S/N ratios are listed in Table 2. The S/N ratio was determined from the sensitivity factor corrected S2p to N1s core-level spectra ratio from Table 1. Comparing the sulfur content of CSA-doped samples with those of DBSA-doped samples, it appears that the S/N ratio of PANI-DBSA (0.637) is higher than PANI-CSA (0.568) with the latter having a closer $[N^+]/[N]$ value (0.567) than the former (0.536). In both blends, the $[N^+]/[N]$ ratio exceeds 50%, which suggests that the strong acid group $-SO_3H$ of two dopants may protonate not only the imine nitrogen but also the amine nitrogen in both complexes. As discussed, there is no possibility of protonating the N atoms of PI on doping. The possible interpretation about possessing a higher $[N^+]/[N]$ value of PANI-CSA may exist in higher acidity of CSA. In the blends, the $[N^+]/[N]$ ratios are visibly different from one another. The CSA-doped blends show higher N^+/N than PANI-CSA, while DBSA-doped blends show lower $[N^+]/[N]$ value than PANI-DBSA. It may be the results of incorporation of carboxylate ion (COO^-) group of PAA that can function as an auxiliary dopant into the PANI chain [22]. Thus, PAA can exist in polymeric anions. It may be suggested that the incorporation of the polymeric anion is more active in PANI-CSA solution than PANI-DBSA solution, because the well defined layered structure of PANI-DBSA should hinder the approach of polymeric anion to the amine nitrogen of PANI. The difficulty in accessibility of carboxylate anion can be also explained in terms of protonation ability. From these results and suppositions, the dopants in the blends seem to have a principle effect on doping level, doping state, and blend behavior because of their pre-formed peculiar morphology.

The imine nitrogen was not shown up to 180°C, which means they were not dedoped until this temperature. Only after the blends cured up to 250°C, the N1s spectra of imine nitrogen appeared in both blends. The proportion of imine nitrogen of C50-250 and D50-250 are 7.2 and 8.9, respectively. It means that the stability to thermal curing of PANI-CSA is higher than PANI-DBSA although the difference is small. The S/N ratio of C50 and D50 are both 0.31, although those of calculated value considering the mole fraction are 0.250 and 0.226, respectively. This coincides well with the S/N ratio of two kinds of PANI-complexes: PANI-DBSA has a higher S content than PANI-CSA. Although S content of 250°C cured samples was decreased, the $[N^+]/[N]$ ratio was increased especially for D50-250.

The UV–Vis spectra of samples, PANI-CSA, PANI-DBSA, PANI-CSA/PAA, PANI-DBSA/PAA, were shown in Figs. 7–10. The samples were cured by step, 120, 150, 180, 210 and 250°C, respectively. Each temperature means the last stage of thermal curing. The UV–Vis spectroscopy spectra of uncured samples show a shoulder-like polaronic peak at around 440 nm and a localized polaron peak over 800 nm [23,24]. The polaron peaks, in other words semiquinone radical cation [25] disappeared after being cured to a high temperature. Clearly, the polaron absorption over 800 nm of pure PANI-complexes (PANI-CSA and PANI-DBSA) disappear when the temperature reaches 210°C, while, that of two kinds of blends disappear only after it reaches 250°C. It can be suggested as follows from these results that blending PANI-complexes with PAA enhances the stability of the chain structure against thermal curing. This is in good accordance with the result that the thermal stability of conductivity of the PANI-complex/PAA blends is superior to pure PANI-complex [3]. But, the disappearing behavior of localized polaron during thermal curing is dissimilar.

Fig. 11 summarizes the movement of the localized polaron peak revealed at about ~800 nm. As the curing temperature increased, this polaron peak gradually shifted to lower wave numbers. This blue shift means the shortening of the conjugation length of PANI or compacted chain structure, which gives rise to defection in conjugation. However, the position of λ_{max} of the localized polaron peak at 180°C increased although it differs from the phase of increasing tendency with the samples except PANI-CSA/PAA which shows only a slightly decreasing phase until 210°C. λ_{max} at 180°C presents a key to the elucidation of

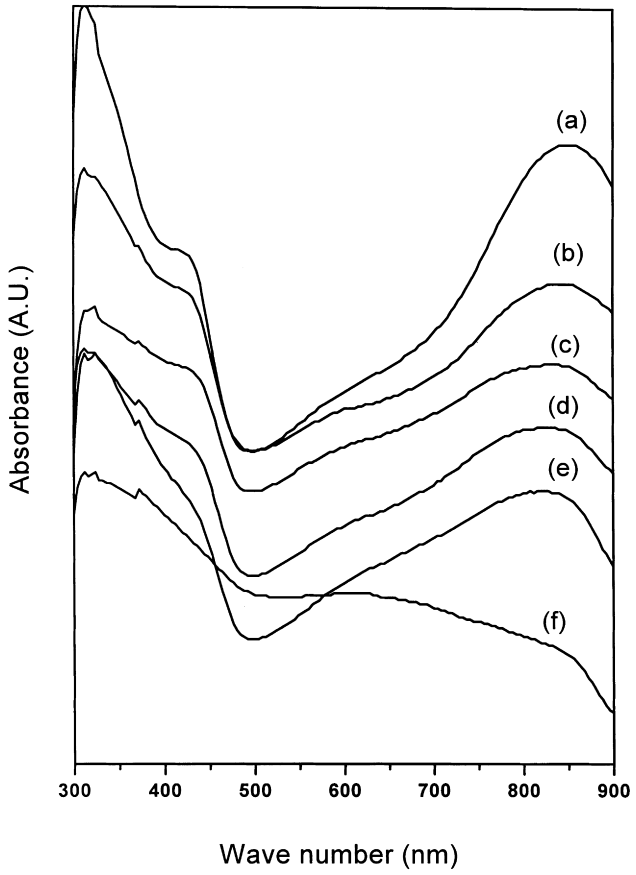

Fig. 8. UV–vis. spectra of C50, and the same material such as those of cured samples: (a) up to proper temperature; (b) 120°C; (c) 150°C; (d) 180°C; (e) 210°C; and (f) 250°C.

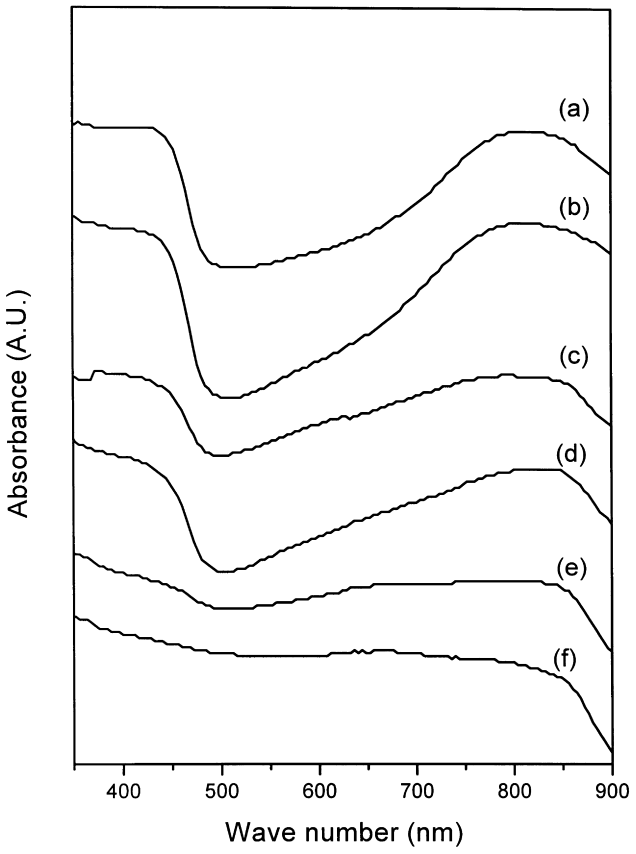

Fig. 9. UV–vis. spectra of PANI-DBSA, and the same material such as those of cured samples: (a) up to proper temperature; (b) 120°C; (c) 150°C; (d) 180°C; (e) 210°C; and (f) 250°C.

the conductivity variance behavior of blends as the thermal treatment step [4]. When the temperature of curing reached 250°C, the polaron peak had completely disappeared and the exciton absorption band at around 600 nm had appeared, indicating that PANI had undergone the dedoping process. Comparing λ_{max} of the localized polaron peak of uncured PANI-complex/PAA blends with pure PANI-complexes and blends show higher values than the PANI-complex in both cases. It may be related with the higher conjugation length of the blends than pure PANI-complex, and that is well agreed with the previously reported conductivity data [3,4]. In these papers, when the PANI content exceeds proper weight content, the conductivity of blends surpassed those of pure PANI-complexes. At 180°C, λ_{max} of all samples except PANI-CSA/PAA are increased. In our previous results, we reported slight increase of conductivity as the thermal curing temperature reaches 180°C. This phenomenon was explained as the annealing effect of the PANI chain by mild thermal treatment. It can also be suggested that the thermal curing affects the chain alignment of the polymer, which leads to the increase of conjugation length and that brings about the increase of conductivity.

Fig. 12 shows the variation of conductivity of the PANI-CSA/PAA and PANI-DBSA/PAA film as a function of temperature. The scanning rate of the temperature is 3°C/min. The conductivity of PANI-CSA/PAA increases slowly until 185°C, and after that temperature it decreases mildly. In the case of PANI-DBSA/PAA, the electrical conductivity decreased steeply after 210°C. It is supposed that the decrease in conductivity can be due to the dissociation or evaporation of dopants from the PANI chain. In light of that, DBSA seems more stable to temperature than CSA. However, the conductivity of DBSA-doped blends drops more steeply than CSA-doped blends after critical temperature (210°C), which also suggested that DBSA dissociate more easily than CSA from the PANI chain after critical temperature. Because of the S (sulfur) content in both blends when the curing temperature of 250°C decreased a bit, many of the dopants that are dissociated from the PANI chain seem to remain in the blends without evaporating. Critical temperatures to which conductivity increased monotonously means that there had to be molecular rearrangement on heating, which made the molecular conformation favorable for electron delocalization. It is in good agreement with the increase of conductivity after mild curing as our previous results [3,4] and again with Fig. 11. The conductivity of PANI-DBSA is higher than that of PANI-CSA at room temperature although the protonation levels of two

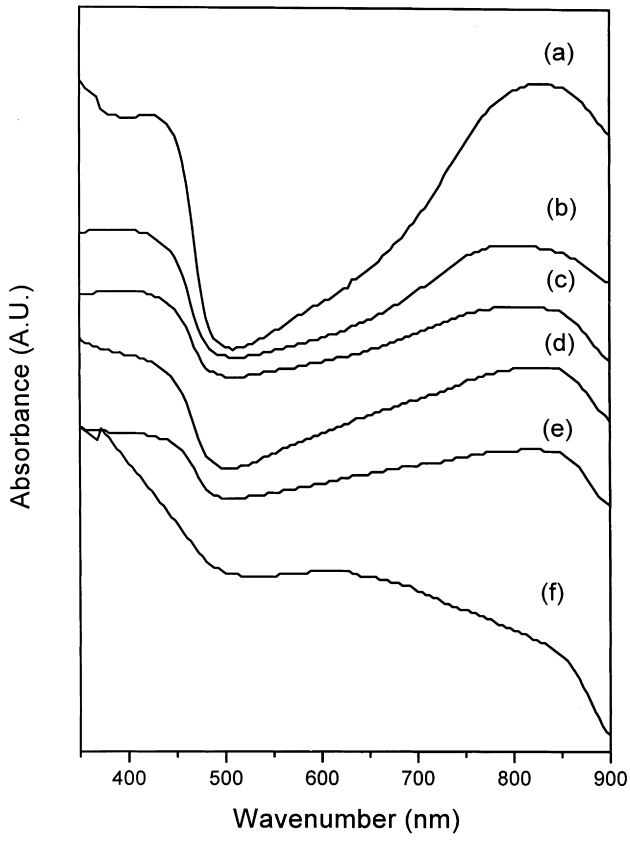

Fig. 10. UV–vis. spectra of D50, and the same material such as those of cured samples: (a) up to proper temperature; (b) 120°C; (c) 150°C; (d) 180°C; (e) 210°C; and (f) 250°C.

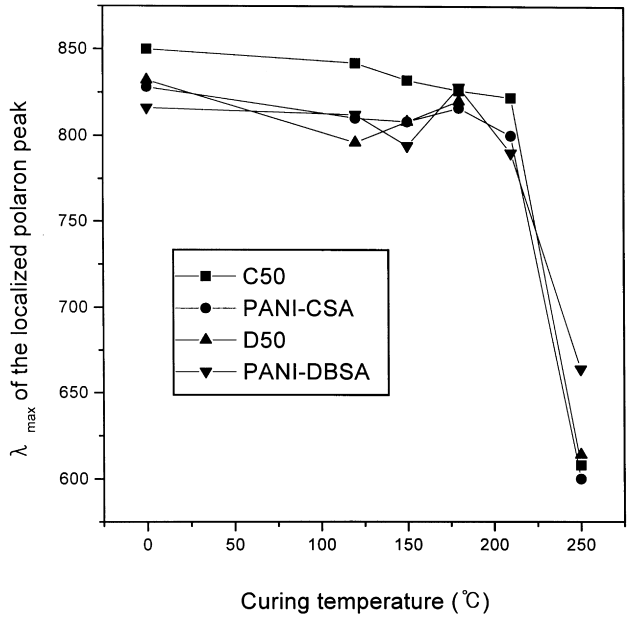

Fig. 11. λ_{max} of the localized polaron peak of all samples as a function of curing temperature.

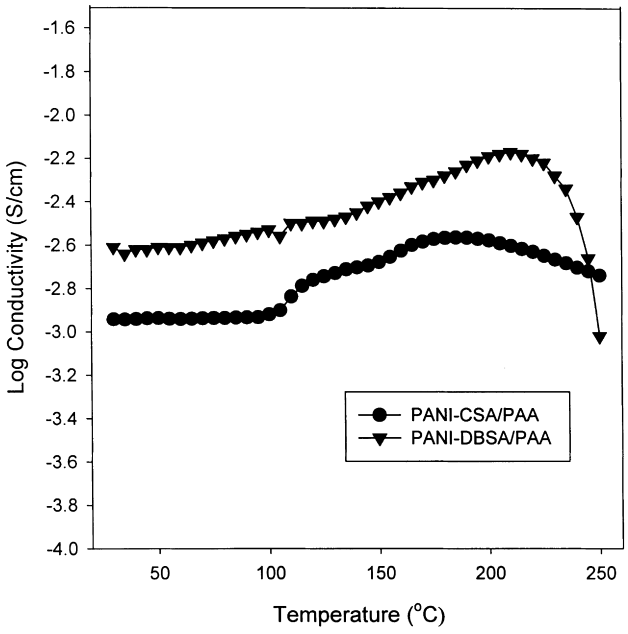

Fig. 12. Log conductivity versus temperature with a heating rate of 3°C/min.

samples are in the other way. It is likely that protonation of amine nitrogens in the emeraldine salt form of PANI and the accompanied conversion of the NH groups to the $-N^{+}H_2-$ groups will interfere with the formation of polarons and bipolarons [26] and result in the interruption of the order of the polaron lattice. That may be the reason for the higher conductivity of DBSA-doped PANI and its blends than CSA-doped PANI and its blends despite the higher doping level of the former.

4. Conclusions

The protonation level, stability of protonation state to thermal curing and the change of conjugation length of our blends were traced by XPS and UV–Vis Spectroscopy measurements. PANI-complexes/PAA and PANI-complexes/PI show that the high doping level exceeded the expected doping level (50%), which may be ascribed to the doping of amine nitrogen in addition to imine nitrogen. The doping level and doping state were the function of dopants in the blends. The imine nitrogen species, which mean dedoped chains are absent, until the curing temperature reached 250°C. DBSA-doped blends show higher content of these imine species after thermal curing at 250°C and lower doping level than CSA-doped blends. But, the electrical conductivity of DBSA-doped blends is somewhat higher than that of CSA-doped blends due to the interference in the formation of polaron in CSA-doped blends owing to excess doping. the thermal stability of protonation levels of blends was higher than that of PANI-complexes. Thermal curing up to 180°C results in

the increase of the conjugation level although the protonation level was relatively low in both blends.

Acknowledgements

The authors acknowledge the financial support of the Korea Research Foundation made in the 1996 program year.

References

[1] Cao Y, Smith P, Heeger AJ. Synth Met 1992;48:91.
[2] Beyer G, Steckenbiegler B. Synth Met 1993;60:169.
[3] Han MG, Im SS. J Appl Polym Sci 1998;67:1863.
[4] Han MG, Im SS. J Appl Polym Sci 1999;71:2169.
[5] Angelopoulos M, Asturias GE, Ermer SP, Ray A, Scherr EM, MacDiarmid AG. Mol Cryst Liq Cryst 1988;160:151.
[6] Chiang JC, MacDiarmid AG. Synth Met 1986;13:193.
[7] Kang ET, Neoh KG, Woo YL, Tan KL, Huan CHA, Wee ATS. Synth Met 1993;53:333.
[8] Li ZF, Kang ET, Neoh KG, Tan KL. Synth Met 1997;87:45.
[9] Kang ET, Li ZF, Neoh KG, Dong YQ, Tan KL. Synth Met 1998;92:167.
[10] Yue J, Epstein AJ. Macromolecules 1991;24:4441.
[11] Aldissi M, Armes SP. Macromolecules 1992;25:2963.
[12] Atanasoska Lj, Anderson SG, Meyer III HM, Lin Z, Weaver JH. J Vac Sci Technol A 1987; 5(6):3325.
[13] Kang ET, Neoh KG, Tan KL. Polymer 1994;35:2899.
[14] Kang ET, Neoh KG, Tan KL. In: Nalwa HS, editor. Handbook of organic conducting molecules and polymers, 3. Chichester: Wiley, 1997, chap. 3.
[15] MacDiarmid AG, Chiang JC, Richter AF, Epstein AJ. Synth Met 1987;18.
[16] Ray A, Asturias GE, Kershner DL, Richter AF, MacDiarmid AG, Epstein AJ. Synth Met 1989;29:E141.
[17] Kang ET, Neoh KG, Tan KL, Tan BTG. Synth Met 1992;46:227.
[18] Nakajima T, Harada M, Osawa R, Kawagoe T, Furukawa Y, Harada I. Macromolecules 1992;22:2664.
[19] Monkman AP, Stevens GG, Bloor DJ. J Physics D: Appl Phys 1991;24:738.
[20] Goh SH, Chan HSO, Ong CH. Polymer 1996;13.
[21] Goh SH, Lee SY, Zhou X. Macromolecules 1998;31:4260.
[22] Angelopoulos M, Patel N, Saraf R. Synth Met 1993;55-57:1522.
[23] Monkman AP, Adams P. Synth Met 1991;40:87.
[24] Stafstrom S, Bredas J, Epstein AJ, Woo HS, Tanner DB, Huang WS, MacDiarmid AG. Phys Rev Lett 1987;59:1464.
[25] Furakawa Y, Ueda F, Hyodo Y, Harada I, Nakajima T, Gawagoe T. Macromolecules 1988;21:1297.
[26] Tanaka K, Wang S, Yamabe T. Synth Met 1990;36:129.